JEM Journal of Experimental Medicine

BRIEF DEFINITIVE REPORT

# Intratumoral accumulation of gut microbiota facilitates CD47-based immunotherapy via STING signaling

Yaoyao Shi[1,2*], Wenxin Zheng[1,2*], Kaiting Yang[1,2], Katharine G. Harris[3], Kaiyuan Ni[4], Lai Xue[1,2,5], Wenbin Lin[1,2,4], Eugene B. Chang[3], Ralph R. Weichselbaum[1,2], and Yang-Xin Fu[6]

**Most studies focus on how intestinal microbiota influence cancer immunotherapy through activating gut immunity. However, immunotherapies related to innate responses such as CD47 blockade rely on the rapid immune responses within the tumor microenvironment. Using one defined anaerobic gut microbiota to track whether microbiota interact with host immunity, we observed that *Bifidobacterium* facilitates local anti-CD47 immunotherapy on tumor tissues through the capacity to accumulate within the tumor microenvironment. Systemic administration of *Bifidobacterium* leads to its accumulation within the tumor and converts the nonresponder mice into responders to anti-CD47 immunotherapy in a stimulator of interferon genes (STING)–and interferon-dependent fashion. Local delivery of *Bifidobacterium* potently stimulates STING signaling and increases cross-priming of dendritic cells after anti-CD47 treatment. Our study identifies the mechanism by which gut microbiota preferentially colonize in tumor sites and facilitate immunotherapy via STING signaling.**

## Introduction

Accumulating evidence suggests that modulating the gut microbiota affects the host responses to various forms of cancer therapy, most notably immunotherapies (Bullman et al., 2017; Geller et al., 2017; Gopalakrishnan et al., 2018; Iida et al., 2013; Matson et al., 2018; Pushalkar et al., 2018; Routy et al., 2018b; Sivan et al., 2015; Vétizou et al., 2015; Viaud et al., 2013; Yu et al., 2017). Recent studies have shown that the diversity and abundance of specific bacterial species influences the therapeutic outcome of blockade of the PD-1/PD-L1 axis (Gopalakrishnan et al., 2018; Matson et al., 2018; Zitvogel et al., 2018). Most of those studies focused on how intestinal microbiota influence cancer immunotherapy through activating gut immunity.

CD47 on tumor cells presents a "don't eat me" signal to macrophages (Chao et al., 2010, 2011). Most studies have focused on how blockade of CD47 improves phagocytosis of the tumor cells by macrophages. Recent studies have also demonstrated a critical role of CD47 blockade to improve cross-presentation in dendritic cells (DCs), thereby connecting innate and adaptive immunity in anti-CD47 immunotherapy (Liu et al., 2015; Xu et al., 2017). CD47 is currently being investigated as a potential therapeutic target for cancer treatment in multiple clinical trials (Advani et al., 2018; Forty Seven, Inc. California Institute for Regenerative Medicine, 2018; Innovent Biologics Co, 2018; Arch Oncology, 2019; Trillium Therapeutics, 2019).

Local administration was reported as an optimal method to enhance antitumor responses by CD47 blockade (Ingram et al., 2017). However, conflicting reports by different laboratories have emerged regarding the antitumor efficacy of anti-CD47 immunotherapy (Chao et al., 2011; Horrigan and Reproducibility Project: Cancer Biology, 2017; Willingham et al., 2012). Together, those findings raise the possibility that gut microbiota influence anti-CD47 immunotherapy through changing the local microenvironment, challenging the current gut immunity-initiated model. Our study identifies the underappreciated mechanism by which gut microbiota preferentially colonize in tumor sites and facilitate immunotherapy via stimulator of interferon genes (STING) signaling at tumor sites instead of regulating gut immunity.

[1]Department of Radiation and Cellular Oncology, University of Chicago, Chicago, IL; [2]The Ludwig Center for Metastasis Research, University of Chicago, Chicago, IL; [3]Department of Medicine, University of Chicago, Chicago, IL; [4]Department of Chemistry, University of Chicago, Chicago, IL; [5]Department of Surgery, University of Chicago, Chicago, IL; [6]Department of Pathology, University of Texas Southwestern Medical Center, Dallas, TX.

*Y. Shi and W. Zheng contributed equally to this paper; Correspondence to Yang-Xin Fu: yang-xin.fu@utsouthwestern.edu; Ralph R. Weichselbaum: rrw@radonc.uchicago.edu.

## Results and discussion

To study whether the antitumor efficacy of CD47 antibody is determined by gut microbiota present in mice, we used WT mice from different facilities, antibiotics-fed mice, and germ-free mice to detect the antitumor efficacy of CD47-based immunotherapy. WT mice from Jackson Laboratory (Jax) and Taconic Biosciences (Tac) were reported to have a distinct gut microbiome that contributes to their distinct immune signatures (Ivanov et al., 2009; Sivan et al., 2015). We observed that tumor-bearing Jax mice responded to CD47 blockade, while tumor-bearing Tac mice failed to respond (Fig. 1 A). To explore whether response to anti-CD47 immunotherapy is attributed to their gut microbiota, we cohoused Jax mice and Tac mice for 3 wk; WT Jax mice and Tac mice responded similarly to CD47 blockade after cohousing (Fig. 1 B). This result indicated that oral transfer or contact transmission of commensal bacteria from mice responders (Jax mice) could sufficiently rescue the antitumor responses in mice nonresponders (Tac mice) to CD47 blockade. To confirm the essential role of gut microbiota in CD47-based immunotherapy, we fed Jax and Tac mice with an antibiotic cocktail before tumor inoculation to reduce the gut microbiota. Jax mice fed with the antibiotic cocktail failed to respond to anti-CD47 therapy (Fig. 1 C). To further confirm that the gut microbiota are essential for the response, germ-free mice were also used (Fig. 1 D). Germ-free mice failed to respond to anti-CD47 antibody treatment. Antibiotic feeding mediated a systemic reduction of microbiota in the whole body. However, the antitumor efficacy of CD47-based immunotherapy relies on the near-complete blockade of CD47 in the tumor microenvironment (TME; Ingram et al., 2017). To specify the location of antitumor effects of gut microbiota that interacted with CD47 blockade, we used very low doses of antibiotic therapy inside tumor tissues. Intratumoral (i.t.) injection of antibiotic cocktail diminished the efficacy of anti-CD47 therapy in mice responders (Fig. 1 E). These findings suggest the efficient role of commensal gut microbes that accumulate outside the gastrointestinal (GI) tract in facilitating CD47-based immunotherapy.

Anaerobic bacteria predominate in the GI tract (Evaldson et al., 1982). The TME becomes more hypoxic as tumor size increases (Fig. 2 A and Fig. S1 A). We hypothesize that hypoxia inside tumor tissues might create a permissive environment for the possible accumulation and growth of anaerobic commensal microbes to enhance innate sensing. Several gut-derived microbial pathogens were detected inside human tumor tissues of the digestive organs, such as colon, liver, and pancreas recently, promoting cancer progression and resistance to antitumor therapies (Bullman et al., 2017; Kimura et al., 1980; Yazawa et al., 2001). *Bifidobacterium* is a commensal anaerobic bacteria that can benefit the conventional treatment of ulcerative colitis and has recently been reported as one functional gut microbiota facilitating PDL1-based immunotherapy via improving the function of DCs (Cui et al., 2003; Furrie et al., 2005; Matson et al., 2018; Sivan et al., 2015; Zitvogel et al., 2018). But how and where *Bifidobacterium* is required for enhancing immunity was not well defined. To track the inner details of how commensal anaerobic bacteria such as *Bifidobacterium* interact with immune cells, Tac mice were administered an i.v. *Bifidobacterium* cocktail (*B. bifidum, B. longum, B. lactis*, and *B. breve*). Surprisingly, *Bifidobacterium* could be readily detected in the tumor tissues 7 d after systemic administration by using anaerobic culture in plates selective for *Bifidobacteria* and 16S ribosomal DNA (rDNA) identification (Fig. 2 B and Fig. S1 B). However, *Bifidobacteria* were not detected in the lung (Fig. 2 B and Fig. S1 B). Although systemic administration of *Bifidobacteria* alone did not control tumor growth, it rescued antitumor efficacy in mice nonresponders to CD47 blockade (Fig. 2 C). This suggests that the tumor-targeting capacity of *Bifidobacterium* is one possible mechanism by which gut microbiota could influence antitumor responses.

To further explore the antitumor role of *Bifidobacteria* accumulation in tumor after systemic delivery, i.t. administration of *Bifidobacteria* was also used. I.t. administration of a much lower dose of *Bifidobacteria* also rescued the capacity of tumor control by CD47 blockade in mice nonresponders bearing colon tumors or lymphoma tumors, consistent with findings in systemic administration of *Bifidobacteria* (Fig. 2, D and E; and Fig. S1 C). It is also possible that more than one type of gut bacteria residing in the TME of Jax mice may facilitate CD47 blockade. These results indicate that the accumulation of *Bifidobacteria* in the TME sufficiently improves the antitumor effects of anti-CD47 immunotherapy.

Oral administration of commensal bacterial as an antitumor strategy has attracted much attention recently (Gopalakrishnan et al., 2018; Matson et al., 2018; Sivan et al., 2015; Zitvogel et al., 2018). Oral administration of a higher dose of *Bifidobacteria* restored the antitumor efficacy of CD47-based immunotherapy in mice nonresponders (Tac mice) and germ-free mice (Fig. 2, F and G). However, oral administration of heat-inactivated bacteria did not exhibit the rescue effect (Fig. S1 D). This result reveals that oral delivery of live *Bifidobacterium* but not inactivated *Bifidobacterium* is sufficient to facilitate the therapeutic effects of the CD47 blockade. On the other hand, *Bifidobacterium* administration synergized with i.t. blockade of CD47 but not systemic blockade of CD47 of a much higher dose (Fig. S1 E). These findings raised the possibility that live *Bifidobacteria* could accumulate in the TME after they were systemically delivered and thereby facilitate the antitumor immunity stimulated by CD47 blockade. Indeed, i.t. administration of a low dose of an antibiotic cocktail sufficiently abrogated the effects of CD47 blockade in mice gavaged with *Bifidobacterium* (Fig. 2 H). The dose of antibiotics did not reduce the *Bifidobacterium* copies in mouse feces (Fig. S1 F). Also, *Bifidobacterium* could be detected in tumor tissues of the mice gavaged with *Bifidobacterium* (Fig. S1 G). These findings confirmed the sufficient role of i.t. *Bifidobacterium* in tumor control by anti-CD47 antibody.

The antitumor efficacy of CD47 blockade was reported to rely on type I IFN signaling and cross-priming of tumor-associated DCs (Liu et al., 2015; Xu et al., 2017). To explore whether *Bifidobacterium* controls type I IFN signaling inside the TME to mediate the therapeutic effects of anti-CD47, we treated mice nonresponders (Tac mice) gavaged with *Bifidobacterium* with a blocking antibody to type I IFN receptor at the tumor sites. I.t. blockade of type I IFN signaling resulted in resistance to CD47 blockade even with *Bifidobacterium* administration (Fig. 3 A). To determine which cell population in the TME requires type I IFN

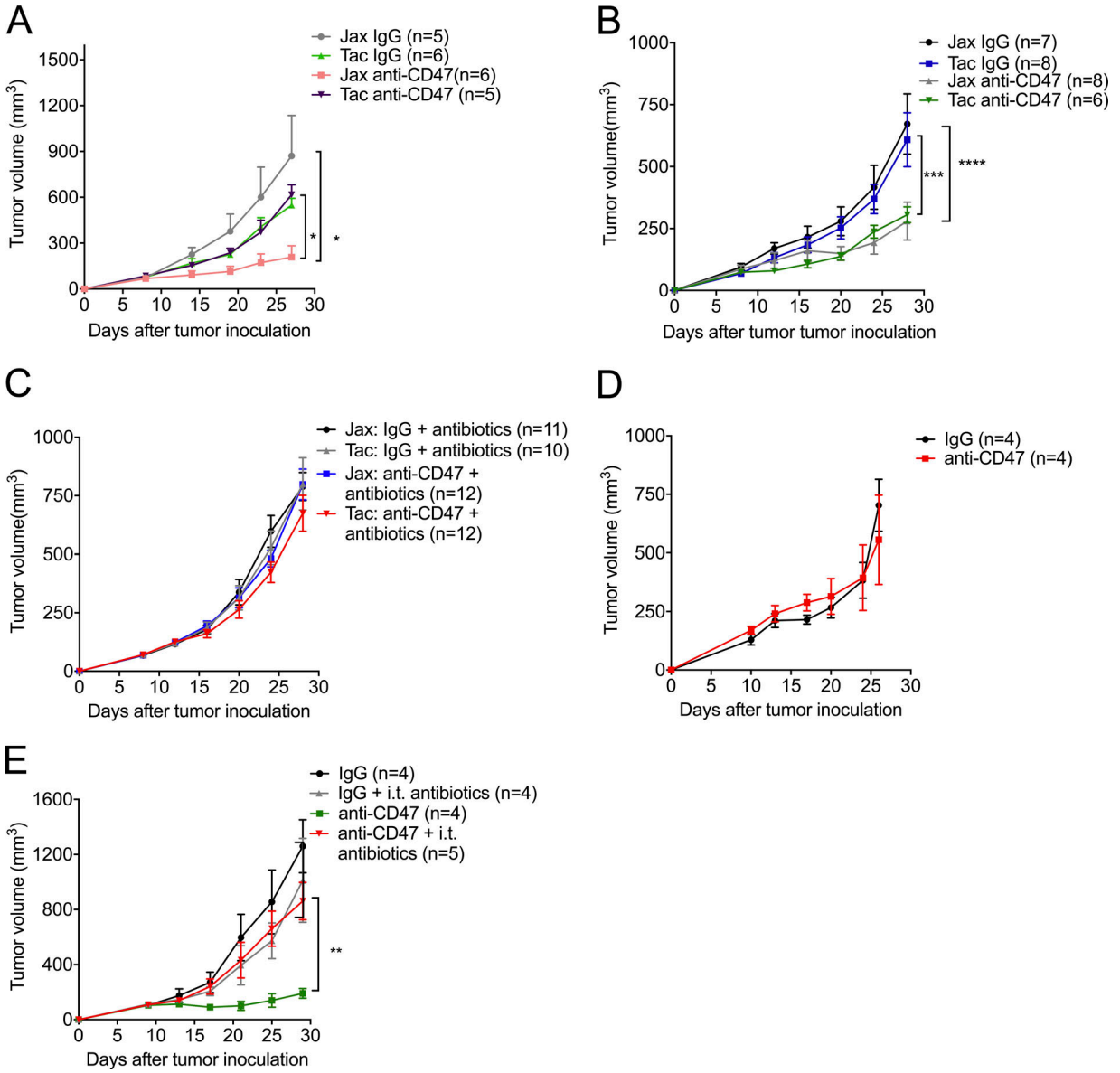


Figure 1. **The antitumor responses of CD47 blockade rely on gut microbiota accumulated outside the GI tract. (A–D)** C57BL/6 mice were injected subcutaneously with 5 × $10^5$ MC38 cells and treated i.t. with 50 µg anti-CD47 antibody (Ab) or rat IgG on days 10 and 14 after tumor inoculation. Tumor volume was measured at indicated time points. **(A)** MC38 tumor growth kinetics in newly arrived Jax and Tac mice treated with anti-CD47 Ab or rat IgG. **(B)** Jax and Tac mice were cohoused for 3 wk before MC38 tumor inoculation and anti-CD47 Ab treatments. **(C)** Jax and Tac mice were given an oral antibiotic cocktail solution (0.5 mg/ml ampicillin, 0.5 mg/ml gentamicin, 0.5 mg/ml metronidazole, 0.5 mg/ml neomycin, and 0.25 mg/ml vancomycin) 3 wk before MC38 tumor inoculation and anti-CD47 Ab treatment and the oral feeding of antibiotics was stopped at the end of the experiments. **(D)** MC38 tumor growth kinetics in germ-free mice treated with anti-CD47 Ab or rat IgG. **(E)** Newly arrived Jax C57BL/6 mice were s.c. injected with 5 × $10^5$ MC38 cells. Each mouse was i.t. injected with 70 µg anti-CD47 Ab or 70 µg rat IgG on day 9 or day 13, respectively. The mice in antibiotics groups were i.t. injected with 100 µl antibiotic cocktail solution every other day. Tumor volume was measured at indicated time points. One representative experiment (A and D) is depicted from at least two experiments yielding similar results. Each group contains at least four mice. Results in C were pooled based on two experiments yielding similar results. Each group contains ≥10 mice. Results in B and E were from one experiment; each group contains at least six (B) and four (E) samples. Presented as mean ± SEM. Two-way ANOVA was used to analyze data in A–E. *, P < 0.05; **, P < 0.01; ***, P < 0.001; ****, P < 0.0001.

signaling for efficient antitumor responses after *Bifidobacterium* administration and CD47 blockade, mice whose *Ifnar* was conditionally knocked out in the DCs were used. Oral administration of *Bifidobacterium* failed to facilitate CD47 blockade in *Ifnar*$^{f/f}$*Cd11c*$^{Cre}$ mice (Fig. 3 B). This finding indicates that type I IFN signaling in DCs is essential for the therapeutic outcome of *Bifidobacterium*-facilitated CD47 blockade. To explore how *Bifidobacterium* influences type I IFN signaling in DCs, the expression of IFNβ was evaluated in isolated tumor DCs. The expression of IFNβ was elevated in tumor DCs from non-responding mice administered with *Bifidobacterium* and anti-CD47, but not mice with only anti-CD47 administration (Fig. 3 C). Similar results were obtained when bone marrow–derived DCs were cocultured with MC38 tumor cells and *Bifidobacterium*

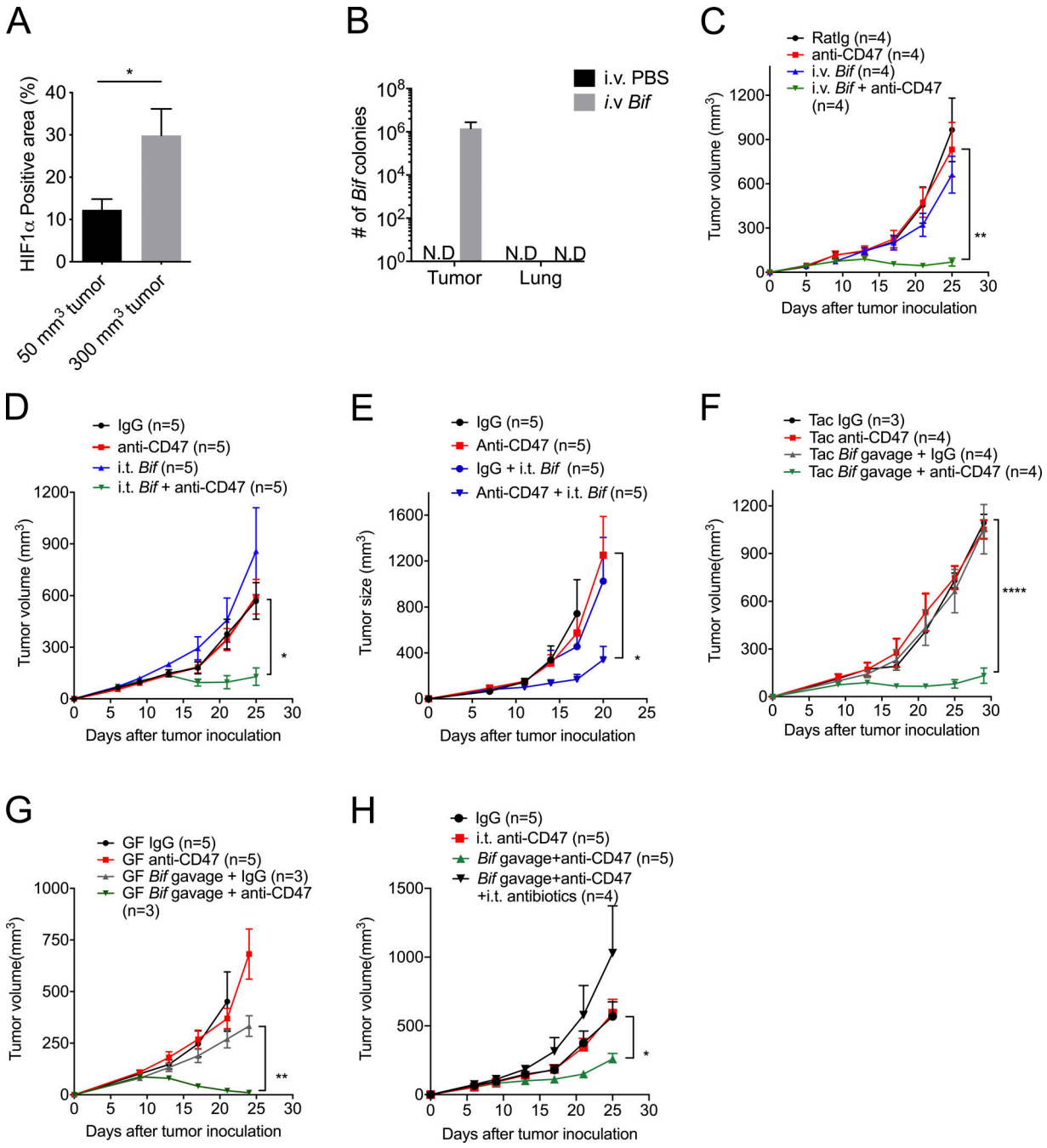


Figure 2. **Administration of *Bifidobacterium*, a tumor-targeting member of the microbiota, sufficiently recovers the antitumor efficacy of anti-CD47 immunotherapy in nonresponders. (A)** Statistical analysis of the percentage of HIF1α-positive area on different-volume tumor tissue slides. **(B)** Detection of *Bifidobacterium* in tumor tissues and lung sites after treatment by anaerobic culture. MC38 tumor–bearing Tac mice were intravenously injected with $1.5 \times 10^7$ CFU activated *Bifidobacterium* three times when tumor sizes approached 200 $mm^3$. 7 d after the final injection, tumor tissues were collected and homogenized for anaerobic culture of *Bifidobacterium*. N.D., not detected. **(C and D)** MC38 tumor–bearing Tac mice were i.t. injected with 70 µg anti-CD47 antibody (Ab) or 70 µg rat IgG on days 9 and 13, respectively. **(C)** Tumor growth kinetics of intravenous injection of *Bifidobacterium*. MC38 tumor-bearing Tac mice were treated with 70 µg anti-CD47 Ab or 70 µg rat IgG on days 9 and 13. For i.v. injection of *Bifidobacterium*, mice were intravenously injected with $1.5 \times 10^7$ CFU *Bifidobacterium* or PBS on the same days on days 6, 9, and 13. **(D)** For i.t. injection of *Bifidobacterium*, mice were i.t. injected with $2.5 \times 10^6$ CFU *Bifidobacterium* or PBS on the same days as i.v. injection of *Bifidobacterium*. The i.t. *Bif* + anti-CD47 group were compared with the IgG group. **(E)** EG7 tumor–bearing TAC mice were treated with 70 µg anti-CD47 Ab or 70 µg rat IgG on days 11 and 13. I.t. injection of $2.5 \times 10^6$ CFU *Bifidobacterium* or PBS was administered on days 8, 11, and 13. Tumor volume was measured at the indicated time points. **(F–H)** Newly arrived Tac C57BL/6 mice (F and H) and germ-free (GF) mice (G) were s.c. injected with $5 \times 10^5$ MC38 cells. Each mouse was i.t. injected with 70 µg anti-CD47 Ab or 70 µg rat IgG on days 9 and 13, respectively. For oral administration of *Bifidobacterium* (*Bif*), mice were gavaged with $5 \times 10^8$ CFU *Bifidobacterium* or PBS on days 6, 9, and 13, respectively. The Tac *Bif* gavage + anti-CD47 group was compared with the Tac IgG group. **(H)** Mice were i.t. injected with 100 µl antibiotic cocktail solution or PBS every other day. Tumor volume was measured at the indicated time points. One representative experiment from at least two experiments yielding similar results is depicted in A–H. Each group in A and B contains at least three samples. The number of mice in each group is depicted in the panels C–H. Presented as mean ± SEM. *, $P < 0.05$ (nonpaired Student's *t* test; A); *, $P < 0.05$; **, $P < 0.01$; ****, $P < 0.0001$ (two-way ANOVA; C–H).

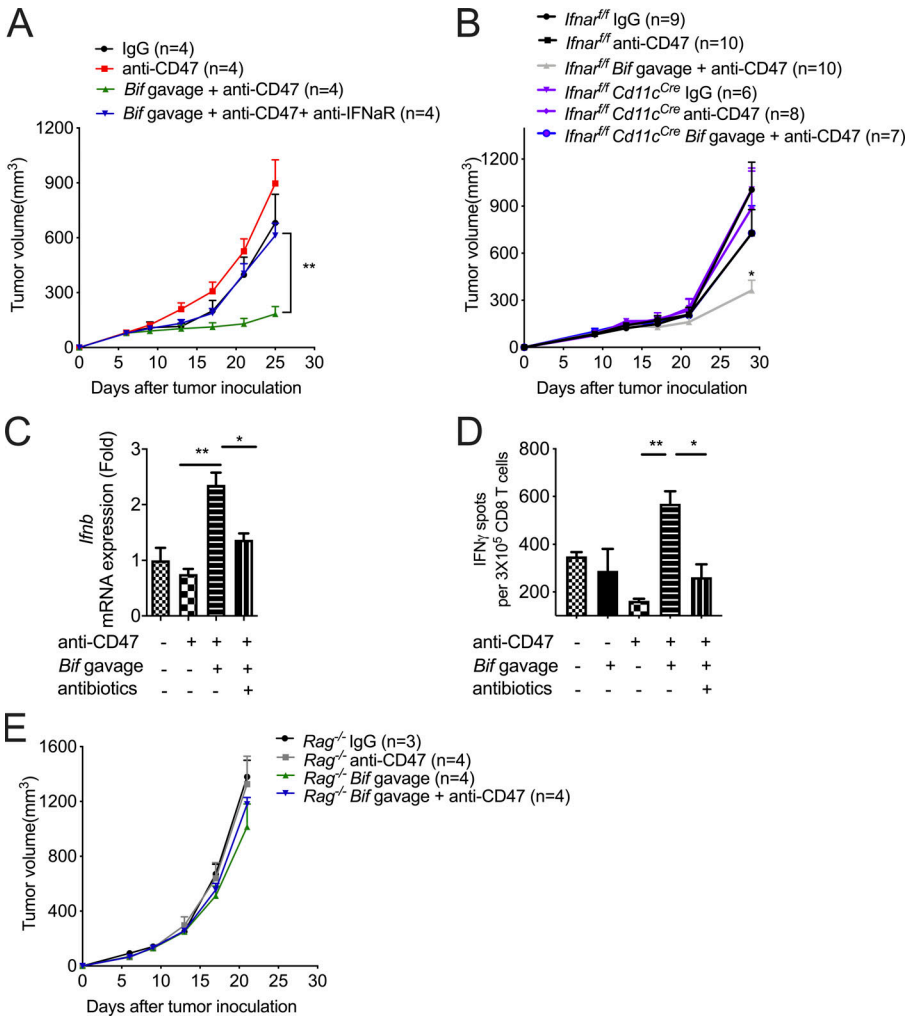


Figure 3. **I.t. type I IFN signaling and T cells are essential for *Bifidobacterium*-mediated tumor control. (A and B)** MC38 tumor–bearing TAC mice (A) and *Ifnar*$^{f/f}$ or *Ifnar*$^{f/f}$*Cd11c*$^{Cre}$ mice (B) were i.t. injected with 70 µg CD47 antibody or 70 µg rat IgG on days 9 and 13. For gavage of *Bifidobacterium*, mice were gavaged with 5 × 10$^8$ *Bifidobacterium* on days 6, 9, and 13. Tumor volume was measured at the indicated time points. **(A)** To block type I IFN signaling, mice were i.t. injected with 200 µg anti-IFNAR or rat IgG on days 6, 8, 10, 12, and 14. The *Bif* gavage + anti-CD47 group is compared with the *Bif* gavage + anti-CD47 + anti-IFNaR group. **(B)** The *Ifnar*$^{f/f}$*Cd11c*$^{Cre}$ *Bif* gavage + anti-CD47 group is compared with the *Ifnar*$^{f/f}$ *Bif* gavage + anti-CD47 group. **(C)** qPCR of *Ifnb1* mRNA levels in tumor-infiltrating DCs. MC38 tumors of TAC mice were injected with 70 µg CD47 antibody or 70 µg rat IgG on day 9. Mouse tumors were injected with 100 µl antibiotic cocktail solution or PBS every other day. For gavage of *Bifidobacterium*, mice were gavaged with 5 × 10$^8$ CFU *Bifidobacterium* on days 6 and 9, respectively. On day 13, tumor tissues were collected for flow cytometric sorting of tumor-infiltrating DCs. *Ifnb1* mRNA levels were quantified by qPCR. **(D)** Number of ELISPOT IFNγ spots of 3 × 10$^5$ sorted OTI-TCR CD8$^+$ T Cells cocultured with DCs from tumor tissues in Tac mice. Tac mice were subcutaneously injected with 2 × 10$^6$ MC38-OTI tumor cells and i.t. injected with 70 µg CD47 antibody or 70 µg rat IgG on days 9 and 12. Mice were i.t. injected with 100 µl antibiotic cocktail solution or PBS every other day from day 6. 2 d after the final injection of antibody, tumor tissues were collected for tumor DC sorting. For gavage of *Bifidobacterium*, mice were gavaged with 5 × 10$^8$ CFU *Bifidobacterium* on days 6, 9, and 12. **(E)** MC38 tumors of *Rag*$^{-/-}$ mice were injected with 70 µg CD47 antibody or 70 µg rat IgG on days 9 and 13. For gavage of *Bifidobacterium*, mice were gavaged with 5 × 10$^8$ CFU *Bifidobacterium* on days 6, 9, and 13. Tumor volume was measured at the indicated time points. One representative experiment from at least two experiments yielding similar results is depicted in A, C, D, and E, and each group contains four mice (A and E). The results in B were based on data pooled from two independent experiments yielding similar results, and each group contains at least six mice. Presented as mean ± SEM. **, P < 0.01 (two-way ANOVA; A and E). *, P < 0.05; **, P < 0.01 (nonpaired Student's *t* test; B, C, and D).

(Fig. S2). On the other hand, i.t. elimination of *Bifidobacterium* by an antibiotic cocktail after oral administration of *Bifidobacterium* decreased the expression of IFNβ in tumor DCs (Fig. 3 C). Taken together, these findings demonstrate that the essential role of type I IFN signaling in the *Bifidobacterium* locally facilitated tumor control by CD47 blockade.

Type I IFN signaling is reported to promote the cross-priming of DCs, which could stimulate adaptive immune responses (Kuchtey et al., 2005; Le Bon et al., 2003). The cross-priming capacity of tumor DCs was evaluated by ELISPOT assay. Increased IFNγ production in CD8$^+$ T cells was elicited only by tumor DCs from the Tac mice receiving both oral administration of *Bifidobacterium* and i.t. injection of anti-CD47 antibody (Fig. 3 D). I.t. elimination of *Bifidobacterium* by an antibiotic cocktail reduced the cross-priming ability of tumor DCs (Fig. 3 D). Furthermore, *Bifidobacterium* administration was unable to restore the antitumor efficacy of CD47 blockade in *Rag*$^{-/-}$ mice (Fig. 3 E). Together, *Bifidobacterium* facilitates CD47-based immunotherapy in an i.t. IFNβ-dependent and T cell–dependent manner.

The stimulator of interferon genes (STING) pathway has been shown to regulate type I IFN expression in the anti-CD47–mediated antitumor effect (Curran et al., 2016; Liu et al., 2015). However, the direct relationship between the STING pathway and the antitumor function of *Bifidobacterium* has not been well defined. We observed that i.t. administration of *Bifidobacterium* failed to facilitate anti-CD47 immunotherapy in *Tmem173*$^{-/-}$ mice, in which mice STING is knocked out (Fig. 4 A). Therefore, STING signaling is essential for the antitumor effects of i.t. *Bifidobacterium*. Similar results were obtained when *Bifidobacterium* was orally delivered to *Tmem173*$^{-/-}$ mice (Fig. 4 B). Oral administration of *Bifidobacterium* also failed to facilitate anti-CD47 immunotherapy in *Tmem173*$^{f/f}$*Cd11c*$^{Cre}$ mice, confirming that the antitumor function of *Bifidobacterium* depended on STING signaling inside DCs (Fig. 4 C). This study suggests that STING agonist targeting on tumor tissues might work well. Indeed, i.t. administration of DMXAA, a murine STING agonist, similarly improved the antitumor efficacy of anti-CD47 therapy in WT TAC mice compared to *Bifidobacterium* (Fig. 4 D).

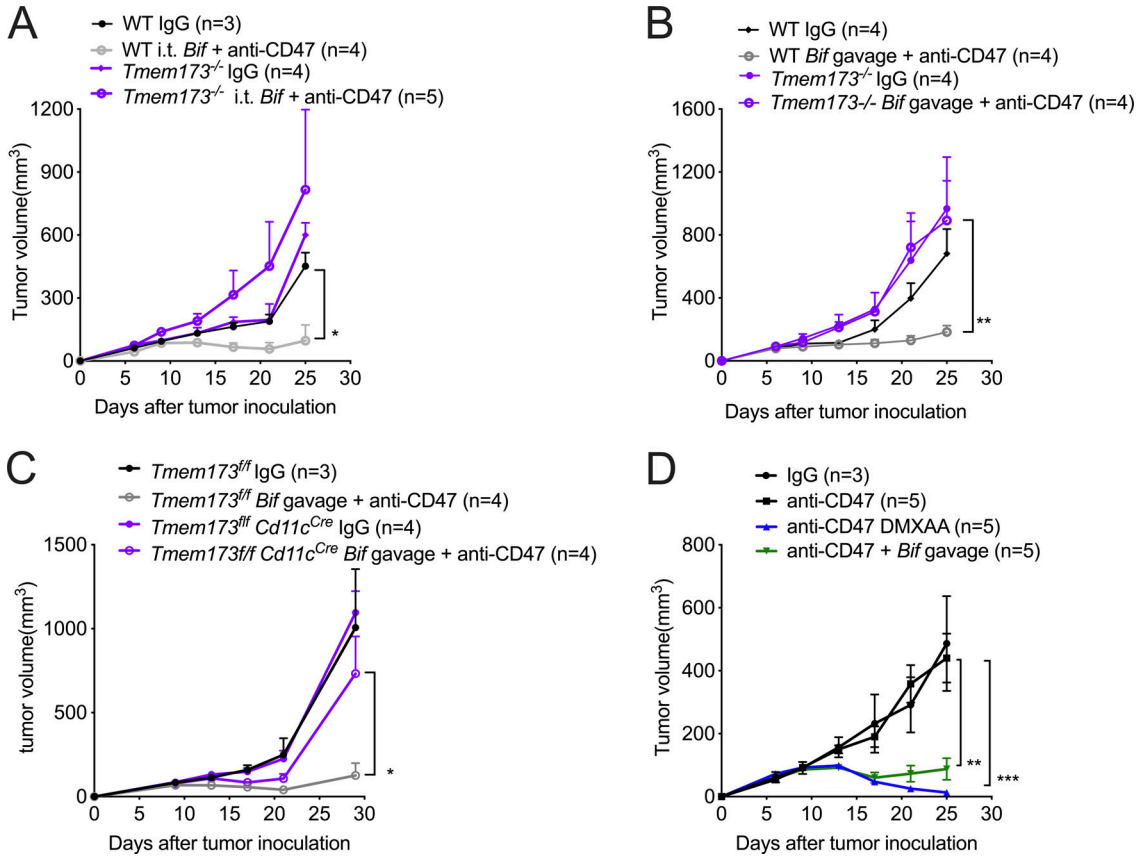


Figure 4. **I.t. *Bifidobacterium* facilitates CD47-based immunotherapy via STING signaling. (A–D)** Mice were injected subcutaneously with 5 × $10^5$ MC38 cells and treated i.t. with 70 µg CD47 antibody or rat IgG on days 9 and 13 after tumor inoculation. Tumor volume was measured at indicated time points. **(A)** Tumor growth kinetics in *Tmem173*$^{-/-}$ mice treated with anti-CD47 antibody (Ab) or rat IgG and i.t. administration of *Bifidobacterium* or PBS. **(B)** Tumor growth kinetics in *Tmem173*$^{-/-}$ mice treated with anti-CD47 Ab or rat IgG and oral administration of *Bifidobacterium* or PBS. The WT *Bif* gavage + anti-CD47 group is compared with the *Tmem173*$^{-/-}$ *Bif* gavage + anti-CD47 group. **(C)** Tumor growth kinetics in *Tmem173*$^{f/f}$ and *Tmem173*$^{f/f}$*Cd11c*$^{Cre}$ mice treated with anti-CD47 Ab or rat IgG and oral administration of *Bifidobacterium* or PBS. The *Tmem173*$^{f/f}$ *Bif* gavage + anti-CD47 group is compared with the *Tmem173*$^{f/f}$ *Cd11c*$^{Cre}$ *Bif* gavage + anti-CD47 group. **(D)** Tumor growth kinetics in Tac C57BL/6 mice treated with anti-CD47 Ab and/or oral administration of *Bifidobacterium*. 20 µg DMXAA were i.t. injected on days 9 and 13. For A–D, one representative experiment from at least two experiments yielding similar results is depicted, and the number of mice per group is depicted in the panels. Presented as mean ± SEM. *, P < 0.05; **, P < 0.01; ***, P < 0.001 (two-way ANOVA; A–D).

The magnitude of efficacy of CD47 blockade is under investigation (Advani et al., 2018; Chao et al., 2010, 2011; Horrigan and Reproducibility Project: Cancer Biology, 2017; Huang et al., 2017; Liu et al., 2015, 2019). In fact, the antitumor efficacy of CD47 varies in preclinical murine models (Horrigan and Reproducibility Project: Cancer Biology, 2017; Liu et al., 2015; Willingham et al., 2012). Improving the responses to CD47 blockade is important to advance its clinical application. Local delivery of low-dose anti-CD47 was observed to be much more effective than systemic delivery of antibody in controlling tumors, raising the possibility that CD47 blockade occurs inside TME. Our study demonstrates that some anaerobic bacteria in the GI tract have tumor-targeting potential and thereby elicit innate and adaptive immune responses sequentially in the TME. *Bifidobacterium* was reported to be overrepresented in the fecal material of JAX mice versus TAC mice, and this correlated with the CD8$^+$ T cell response (Sivan et al., 2015). Using *Bifidobacterium,* a well-defined commensal probiotic that influences immunotherapy, for better tracking, we observed that this anaerobic member of the microbiota could actually localize to the TME and facilitate CD47-based immunotherapy via STING signaling. Other bacteria such as *Akkermansia* and *Faecalibacterium* have also been reported as beneficial to checkpoint immunotherapies (Cani and de Vos, 2017; Jobin, 2018; Routy et al., 2018a; Zhou et al., 2018b). It is very possible that more than one type of anerobic gut microbiota is tumor targeting and enhances immunity inside TME. It will be interesting to determine whether these bacteria can also localize in the TME and conduct their antitumor function related to anti-CD47 immunotherapies.

Our study demonstrates that a specific member of the gut microbiota enhances the antitumor efficacy of immunotherapy by colonizing in the tumor sites. Therefore, i.t. administration of specific bacterial species or their engineered progenies may be a novel and effective strategy to modulate various antitumor immunotherapies and act as a powerful adjuvant to surgery and radiotherapy. Several studies using *Salmonella typhimurium* or *Clostridium novyi-NT* as tumor targeting bacteria are being tested in ongoing clinical trials (Zhou et al., 2018a), but their pathogenicity might be difficult to manage. Here, we showed that *Bifidobacterium*, an anaerobic commensal bacterium residing in

the GI tract, can colonize inside the tumor and modulate the immune response elicited by CD47 blockade. Given that *Bifidobacterium* is a commensal bacterium with low toxicity and low chance of survival in normal tissues, it can be a good tumor-targeting bacteria for clinical translation.

Live bacteria actively migrate and continually produce secondary metabolites to trigger the STING pathway inside DCs. The synergistic role between bacterial STING agonists and the cGAS product cGAMP for STING activation is intriguing and needs to be further explored. Whether other bacterial products produced by *Bifidobacterium* can also facilitate host responses remains to be determined. The checkpoint blockade immunotherapies target T cells directly. These bacteria products improve the antigen-presenting capacity of DCs and elicit robust adaptive immune responses. Therefore, these bacterial metabolites may also synergize with other T cell–targeted immunotherapies. Our study opens a new avenue for investigation in clinical practice regarding the microbiome inside TME that synergizes with immunotherapy and unravels the situation that some patients fail to respond to immunotherapy.

## Materials and methods

### Animals and tumor model

5- or 7-wk-old C57BL/6 mice were purchased from Jackson Laboratory or Taconic Biosciences. 5- or 6-wk-old Balb/c mice were purchased from Taconic Biosciences. *Tmem173*$^{-/-}$, OT-I CD8$^{+}$ TCR-Tg, *Cd11c*$^{Cre}$ mice were purchased from Jackson Laboratory. *Ifnar*$^{flox/flox}$ mice were kindly provided by Dr. Ulrich Kalinke from the Institute for Experimental Infection Research, Hanover, Germany. *Tmem173*$^{flox/flox}$ mice were kindly provided by Dr. John Cambier from National Jewish Health, Denver, CO. All the mice were maintained under specific pathogen–free (SPF) conditions in accordance with the animal experimental guidelines set by the Institutional Animal Care and Use Committee at the University of Chicago. Germ-free C56BL/6 mice were initially obtained from Taconic Biosciences and maintained in flexible-film isolators in the University of Chicago Gnotobiotic Research Animal Facility. Female mice were used for experiments unless specified otherwise. MC38 is a murine colon adenocarcinoma cell line. EG7 is a murine T cell lymphoma cell line. MC38-OTI peptide cells were sorted and subcloned after MC38 cells were transduced with lentivirus expressing OT-I peptide. A list of reagents and resources is included in Table S1.

### Anti-CD47 mAb immunotherapy and treatments

For anti-CD47 antibody injection, mice were injected i.t. with 50–70 µg anti-CD47 (clone MIAP301, BioXCell) 9 or 10 d and 13 or 14 d after tumor inoculation. For anti-CD47 antibody systemic injection, mice were injected i.p. with 500 µg anti-CD47 9 d and 13 d after tumor inoculation. For anti-IFNαR antibody injection, mice were injected i.t. with 200 µg anti-IFNαR antibody 6, 8, 10, 12, and 14 d after tumor inoculation. For DMXAA administration, mice were injected i.t. with 20 µg DMXAA either 9 or 13 d after tumor inoculation.

### Bacteria administration and heat inactivation

For bacteria oral administration, germ-free mice or SPF C57BL/6 mice were gavaged with 5 × 10$^{8}$ CFU *Bifidobacterium* species mix (*B. bifidum*, *B. longum*, *B. lactis*, and *B. breve*, Seeking Health) 6, 9, or 13 d after tumor inoculation. For bacteria systemic administration, SPF C57BL/6 mice were injected i.v. with 1.5 × 10$^{7}$ CFU *Bifidobacterium* species mix 6, 9, or 13 d after tumor inoculation. For bacterial i.t. administration, SPF C57BL/6 mice were injected i.t. with 2.5 × 10$^{6}$ CFU *Bifidobacterium* species mix 6, 9, or 13 d after tumor inoculation. Heat inactivation was performed by boiling *Bifidobacterium* at 100°C for 2 h.

### Antibiotic administration

For antibiotic oral administration, Jax or Tac mice started to be fed with antibiotic suspensions (0.5 mg/ml ampicillin, 0.5 mg/ml gentamicin, 0.5 mg/ml metronidazole, 0.5 mg/ml neomycin, and 0.25 mg/ml vancomycin dissolved in autoclaved water) 3 wk before tumor inoculation, and received them until end points. All the antibiotics were purchased from Sigma-Aldrich. For antibiotic i.t. administration, TAC mice were injected i.t. with 100 µl antibiotic suspensions every other day after oral administration of *Bifidobacterium*, and ending 4 d after the final oral administration of *Bifidobacterium*.

### Bacterial quantification in the tumor, organs, and fecal samples

For bacterial colony assay, tumor and organ tissues were sterilely collected and homogenized in 3 or 5 ml sterile PBS supplemented with 0.05% cysteine-HCl. After dilution, 100-µl tissue suspensions were plated on reinforced clostridial agar (Sigma-Aldrich) containing 50 mg/liter mupirocin. Resulting colonies were confirmed by 16S rDNA quantitative PCR (qPCR) and used to calculate the number of *Bifidobacterium* cells per tissue sample. For 16S rDNA qPCR quantification, fecal and tissue samples were collected and homogenized. Total DNA was extracted by QIAamp PowerFecal DNA kit (Qiagen, 12830-50). Primer sets included two primers, BifidF (5′-CGGGTGAGTAATGCGTGACC-3′) and BifidR (5′-TGATAGGACGCGACCCCA-3′), and one probe (5′-6FAM-CTCCTGGAAACGGGTG-3′; Sivan et al., 2015). Primers and probe were synthesized by Invitrogen. Real-time qPCR was performed by using TaqMan Universal qPCR 2x Master Mix (Applied Biosystems).

### DC sorting and IFNγ ELISPOT

For quantification of *Ifnb1* mRNA, MC38 tumor–bearing Tac C57BL/6 mice were injected i.t. with 70 µg of rat IgG or CD47 antibody on day 9. Mice were injected i.t. with 100 µl antibiotic cocktail solution or PBS every other day. For gavage of *Bifidobacterium*, mice were gavaged with 5 × 10$^{8}$ CFU *Bifidobacterium* on days 6 and 9. On day 13, tumor tissues were collected for flow cytometric sorting of tumor-infiltrating DCs. Tumor tissues were excised and digested by 50 µg/ml Liberase TM (Roche). Single-cell suspensions were blocked by anti-FcR (clone 2.4G2, BioXCell) and stained with anti-CD45 (clone 30-F11, BioLegend), anti-CD11c (clone N418, BioLegend), anti-F4/80 (clone BM8, eBioscience), anti-CD11b (M1/70, BioLegend), and anti-MHC II (M5/114.15.2, BioLegend) antibodies. CD45$^{+}$CD11c$^{+}$ CD11b$^{+/-}$F4/80$^{-}$MHCII$^{high}$ tumor-infiltrating DCs were sorted with a FACs Aria IIIu Cell Sorter (BD). *Ifnb1* mRNA levels were quantified by qPCR.

For IFN-γ Elispot, MC38-OTI tumor–bearing Tac C57BL/6 mice were injected i.t. with 70 µg of rat IgG or anti-CD47 antibody on days 9 and 12. Mice were injected i.t. with 100 µl antibiotic cocktail solution or PBS every other day from day 6. 2 d after the final injection of antibody, tumor tissues and draining lymph nodes were collected for tumor DC sorting. For gavage of *Bifidobacterium*, mice were gavaged with $5 \times 10^8$ *Bifidobacterium* on days 6, 9, and 12. Approximately $5 \times 10^4$ DCs were mixed together with purified $3 \times 10^5$ OTI-TCR $CD8^+$ T cells for 3 d, and then IFNγ-producing cells were enumerated by ELISPOT assay.

### In vitro assay of bone marrow–derived DCs

Bone marrow–derived DCs ($2 \times 10^6$) were cocultured with MC38 cells ($2 \times 10^6$) with 10 µg/ml anti-CD47 or 10 µg/ml rat IgG in the presence or absence of $2 \times 10^6$ *Bifidobacterium* for 8 h. DCs were then sorted out for *Ifnb1* quantification by qPCR. In some experiments, $2 \times 10^6$ bone marrow–derived DCs were cocultured with $2 \times 10^6$ *Bifidobacterium*, heated-killed *Bifidobacterium*, or *Bifidobacterium* culture supernatants (1:10 diluted), respectively. The resulting supernatants were collected 16 h later, followed by quantification of IFNβ concentration with VeriKine-HS Mouse Interferon Beta Serum ELISA Kit (PBL Assay Science) in accordance with the manufacturer's instructions.

### HIF-1α immunofluorescence staining

Hypoxia levels were evaluated by the ab190197 antibody conjugated with Alexa Fluor 488 fluorochrome against HIF-1α (Abcam) ex vivo. For immunofluorescence imaging, MC38 tumor–bearing mice were sacrificed, and tumors and hearts were excised with Cryostat (Leica). The sections were air-dried for ≥1 h and then fixed in acetone for 10 min at 20°C. After staining with Alexa Fluor 488–HIF-1α and DAPI, these sections were washed twice with PBS and observed and scanned with a FV1000 confocal laser scanning microscope (Olympus) and Caliber RS-G4 Upright confocal microscope (Caliber I.D.). Images were further processed and analyzed with ImageJ software (National Institutes of Health).

### qPCR

Total RNA from sorted tumor-infiltrating DCs or cocultured DCs was extracted by using the RNeasy Plus Mini Kit (Qiagen, 74134) and reversed-transcribed with Applied Biosystems High-Capacity cDNA Reverse Transcription Kit (Thermo Fisher Scientific, 4368814). *Ifnb* primers include *Infb* forward (5′-TGAACTCCA CCAGCAGACA-3′) and reverse (5′-ACCACCATCCAGGCGTAG-3′); *Gapdh* primers include *Gapdh* forward (5′-AGGTCGGTG TGAACGGATTTG-3′) and reverse (5′-TGTAGACCATGTAGT TGAGGTCA-3′). Real-time qPCR was performed by using Applied Biosystems Power SYBR Green PCR master mix (Thermo Fisher Scientific, 43-687-02) according to the manufacturer's instructions. Data were normalized to the RNA level of *Gapdh*. 2–ΔΔCt method was used to calculate the relative expression changes.

### Statistical analysis

For all mouse studies, mice were grouped at random and, if possible, mixed among different cages. Tumor growth curves were analyzed using two-way ANOVA and are presented as mean values ± SEM. For other comparisons, unpaired Student's *t* test was used if two groups were compared. $P < 0.05$ was considered statistically significant and denoted as follows: *, $P < 0.05$; **, $P < 0.01$; ***, $P < 0.001$; and ****, $P < 0.0001$. Statistical analysis was performed using Graphpad Prism.

### Online supplemental material

Fig. S1 shows the representative immunofluorescence images of the tumor hypoxia sites, the 16S QPCR results of tissue-residing *Bifidobacterium*, increased survival rates by administration of anti-CD47 and *Bifidobacterium*, the antitumor efficacy of heat-killed *Bifidobacterium* or systemic injection of anti-CD47 antibody, and the number of *Bifidobacterium* in feces and tumor tissues after i.t. injection of antibiotic cocktail. Fig. S2 shows that *Bifidobacterium* could collaborate with anti-CD47 to up-regulate the expression of IFNβ in DCs cocultured with tumor cells in vitro. Table S1 shows the sources of all the reagents and resources used.

## Acknowledgments

We thank Hua Liang, Meng Xu, Yuzhu Hou, Ainhoa Arina, Diana Ranoa, and Sean Pitroda for helpful discussion; Amy Huser for excellent editing; and David Leclerc, Candace Cam, and Jason Koval for technical assistance.

This work was supported by a grant from the Ludwig Foundation to R.R. Weichselbaum, a generous gift from the Foglia Foundation (Y-X. Fu and R.R. Weichselbaum), and National Institutes of Health/National Cancer Institute Provocative Questions grant R21 CA231273-01 (R.R. Weichselbaum) and CA141975, and Cancer Prevention and Research Institute of Texas grants RR150072 and RP 180725 (Y-X. Fu).

Author contributions: Y. Shi, W. Zheng, R.R. Weichselbaum, and Y-X. Fu conceived and designed the study; Y. Shi, W. Zheng, K. Yang, K.G. Harris, K. Ni, and L. Xue performed the experiments. W. Lin and E.B. Chang contributed resources. Y. Shi and W. Zheng analyzed the data. Y. Shi wrote the manuscript. W. Zheng, R.R. Weichselbaum, and Y-X. Fu edited the manuscript. R.R. Weichselbaum and Y-X. Fu provided guidance for the research.

Disclosures: The authors declare no competing interests exist.

Submitted: 4 December 2019
Revised: 10 January 2020
Accepted: 22 January 2020

## References

Advani, R., I. Flinn, L. Popplewell, A. Forero, N.L. Bartlett, N. Ghosh, J. Kline, M. Roschewski, A. LaCasce, G.P. Collins, et al. 2018. CD47 Blockade by Hu5F9-G4 and Rituximab in Non-Hodgkin's Lymphoma. *N. Engl. J. Med.* 379:1711–1721. https://doi.org/10.1056/NEJMoa1807315

Arch Oncology. 2019. AO-176 in Multiple Solid Tumor Malignancies. Available at: https://ichgcp.net/clinical-trials-registry/NCT03834948.

Bullman, S., C.S. Pedamallu, E. Sicinska, T.E. Clancy, X. Zhang, D. Cai, D. Neuberg, K. Huang, F. Guevara, T. Nelson, et al. 2017. Analysis of

*Fusobacterium* persistence and antibiotic response in colorectal cancer. *Science.* 358:1443–1448. https://doi.org/10.1126/science.aal5240

Cani, P.D., and W.M. de Vos. 2017. Next-Generation Beneficial Microbes: The Case of *Akkermansia muciniphila*. *Front. Microbiol.* 8:1765. https://doi.org/10.3389/fmicb.2017.01765

Chao, M.P., A.A. Alizadeh, C. Tang, J.H. Myklebust, B. Varghese, S. Gill, M. Jan, A.C. Cha, C.K. Chan, B.T. Tan, et al. 2010. Anti-CD47 antibody synergizes with rituximab to promote phagocytosis and eradicate non-Hodgkin lymphoma. *Cell.* 142:699–713. https://doi.org/10.1016/j.cell.2010.07.044

Chao, M.P., A.A. Alizadeh, C. Tang, M. Jan, R. Weissman-Tsukamoto, F. Zhao, C.Y. Park, I.L. Weissman, and R. Majeti. 2011. Therapeutic antibody targeting of CD47 eliminates human acute lymphoblastic leukemia. *Cancer Res.* 71:1374–1384. https://doi.org/10.1158/0008-5472.CAN-10-2238

Cui, H.H., C.L. Chen, J.D. Wang, Y.J. Yang, Y. Sun, Y.D. Wang, and Z.S. Lai. 2003. [The effects of bifidobacterium on the intestinal mucosa of the patients with ulcerative colitis]. *Zhonghua Nei Ke Za Zhi.* 42:554–557.

Curran, E., X. Chen, L. Corrales, D.E. Kline, T.W. Dubensky Jr., P. Duttagupta, M. Kortylewski, and J. Kline. 2016. STING Pathway Activation Stimulates Potent Immunity against Acute Myeloid Leukemia. *Cell Reports.* 15:2357–2366. https://doi.org/10.1016/j.celrep.2016.05.023

Evaldson, G., A. Heimdahl, L. Kager, and C.E. Nord. 1982. The normal human anaerobic microflora. *Scand. J. Infect. Dis. Suppl.* 35:9–15.

Forty Seven, Inc. California Institute for Regenerative Medicine. 2018. CAMELLIA: Anti-CD47 Antibody Therapy in Haematological Malignancies. Available at: https://clinicaltrials.gov/ct2/show/NCT02678338.

Furrie, E., S. Macfarlane, A. Kennedy, J.H. Cummings, S.V. Walsh, D.A. O'neil, and G.T. Macfarlane. 2005. Synbiotic therapy (Bifidobacterium longum/Synergy 1) initiates resolution of inflammation in patients with active ulcerative colitis: a randomised controlled pilot trial. *Gut.* 54:242–249. https://doi.org/10.1136/gut.2004.044834

Geller, L.T., M. Barzily-Rokni, T. Danino, O.H. Jonas, N. Shental, D. Nejman, N. Gavert, Y. Zwang, Z.A. Cooper, K. Shee, et al. 2017. Potential role of intratumor bacteria in mediating tumor resistance to the chemotherapeutic drug gemcitabine. *Science.* 357:1156–1160. https://doi.org/10.1126/science.aah5043

Gopalakrishnan, V., C.N. Spencer, L. Nezi, A. Reuben, M.C. Andrews, T.V. Karpinets, P.A. Prieto, D. Vicente, K. Hoffman, S.C. Wei, et al. 2018. Gut microbiome modulates response to anti-PD-1 immunotherapy in melanoma patients. *Science.* 359:97–103. https://doi.org/10.1126/science.aan4236

Horrigan, S.K. Reproducibility Project: Cancer Biology. 2017. Replication Study: The CD47-signal regulatory protein alpha (SIRPa) interaction is a therapeutic target for human solid tumors. *eLife.* 6:e18173. https://doi.org/10.7554/eLife.18173

Huang, Y., Y. Ma, P. Gao, and Z. Yao. 2017. Targeting CD47: the achievements and concerns of current studies on cancer immunotherapy. *J. Thorac. Dis.* 9:E168–E174. https://doi.org/10.21037/jtd.2017.02.30

Iida, N., A. Dzutsev, C.A. Stewart, L. Smith, N. Bouladoux, R.A. Weingarten, D.A. Molina, R. Salcedo, T. Back, S. Cramer, et al. 2013. Commensal bacteria control cancer response to therapy by modulating the tumor microenvironment. *Science.* 342:967–970. https://doi.org/10.1126/science.1240527

Ingram, J.R., O.S. Blomberg, J.T. Sockolosky, L. Ali, F.I. Schmidt, N. Pishesha, C. Espinosa, S.K. Dougan, K.C. Garcia, H.L. Ploegh, and M. Dougan. 2017. Localized CD47 blockade enhances immunotherapy for murine melanoma. *Proc. Natl. Acad. Sci. USA.* 114:10184–10189. https://doi.org/10.1073/pnas.1710776114

Innovent Biologics Co. 2018. A Phase 1 Study Evaluating the Safety, Tolerability, and Initial Efficacy of Recombinant Human Anti-cluster Differentiation Antigen 47 (CD47) Monoclonal Antibody Injection (IBI188) in Patients With Advanced Malignancies. Available at: https://clinicaltrials.gov/ct2/show/NCT03717103.

Ivanov, I.I., K. Atarashi, N. Manel, E.L. Brodie, T. Shima, U. Karaoz, D. Wei, K.C. Goldfarb, C.A. Santee, S.V. Lynch, et al. 2009. Induction of intestinal Th17 cells by segmented filamentous bacteria. *Cell.* 139:485–498. https://doi.org/10.1016/j.cell.2009.09.033

Jobin, C. 2018. Precision medicine using microbiota. *Science.* 359:32–34. https://doi.org/10.1126/science.aar2946

Kimura, N.T., S. Taniguchi, K. Aoki, and T. Baba. 1980. Selective localization and growth of Bifidobacterium bifidum in mouse tumors following intravenous administration. *Cancer Res.* 40:2061–2068.

Kuchtey, J., P.J. Chefalo, R.C. Gray, L. Ramachandra, and C.V. Harding. 2005. Enhancement of dendritic cell antigen cross-presentation by CpG DNA involves type I IFN and stabilization of class I MHC mRNA. *J. Immunol.* 175:2244–2251. https://doi.org/10.4049/jimmunol.175.4.2244

Le Bon, A., N. Etchart, C. Rossmann, M. Ashton, S. Hou, D. Gewert, P. Borrow, and D.F. Tough. 2003. Cross-priming of CD8+ T cells stimulated by virus-induced type I interferon. *Nat. Immunol.* 4:1009–1015. https://doi.org/10.1038/ni978

Liu, X., Y. Pu, K. Cron, L. Deng, J. Kline, W.A. Frazier, H. Xu, H. Peng, Y.X. Fu, and M.M. Xu. 2015. CD47 blockade triggers T cell-mediated destruction of immunogenic tumors. *Nat. Med.* 21:1209–1215. https://doi.org/10.1038/nm.3931

Liu, X., X. Wu, Y. Wang, Y. Li, X. Chen, W. Yang, and L. Jiang. 2019. CD47 promotes human glioblastoma invasion through activation of PI3K/Akt pathway. *Oncol. Res.* 27:415–422.

Matson, V., J. Fessler, R. Bao, T. Chongsuwat, Y. Zha, M.L. Alegre, J.J. Luke, and T.F. Gajewski. 2018. The commensal microbiome is associated with anti-PD-1 efficacy in metastatic melanoma patients. *Science.* 359:104–108. https://doi.org/10.1126/science.aao3290

Pushalkar, S., M. Hundeyin, D. Daley, C.P. Zambirinis, E. Kurz, A. Mishra, N. Mohan, B. Aykut, M. Usyk, L.E. Torres, et al. 2018. The Pancreatic Cancer Microbiome Promotes Oncogenesis by Induction of Innate and Adaptive Immune Suppression. *Cancer Discov.* 8:403–416. https://doi.org/10.1158/2159-8290.CD-17-1134

Routy, B., V. Gopalakrishnan, R. Daillère, L. Zitvogel, J.A. Wargo, and G. Kroemer. 2018a. The gut microbiota influences anticancer immunosurveillance and general health. *Nat. Rev. Clin. Oncol.* 15:382–396. https://doi.org/10.1038/s41571-018-0006-2

Routy, B., E. Le Chatelier, L. Derosa, C.P.M. Duong, M.T. Alou, R. Daillère, A. Fluckiger, M. Messaoudene, C. Rauber, M.P. Roberti, et al. 2018b. Gut microbiome influences efficacy of PD-1-based immunotherapy against epithelial tumors. *Science.* 359:91–97. https://doi.org/10.1126/science.aan3706

Sivan, A., L. Corrales, N. Hubert, J.B. Williams, K. Aquino-Michaels, Z.M. Earley, F.W. Benyamin, Y.M. Lei, B. Jabri, M.-L. Alegre, et al. 2015. Commensal Bifidobacterium promotes antitumor immunity and facilitates anti-PD-L1 efficacy. *Science.* 350:1084–1089. https://doi.org/10.1126/science.aac4255

Trillium Therapeutics. 2019. A Trial of TTI-621 for Patients With Hematologic Malignancies and Selected Solid Tumors. Available at: https://clinicaltrials.gov/ct2/show/NCT02663518.

Vétizou, M., J.M. Pitt, R. Daillère, P. Lepage, N. Waldschmitt, C. Flament, S. Rusakiewicz, B. Routy, M.P. Roberti, C.P.M. Duong, et al. 2015. Anticancer immunotherapy by CTLA-4 blockade relies on the gut microbiota. *Science.* 350:1079–1084. https://doi.org/10.1126/science.aad1329

Viaud, S., F. Saccheri, G. Mignot, T. Yamazaki, R. Daillère, D. Hannani, D.P. Enot, C. Pfirschke, C. Engblom, M.J. Pittet, et al. 2013. The intestinal microbiota modulates the anticancer immune effects of cyclophosphamide. *Science.* 342:971–976. https://doi.org/10.1126/science.1240537

Willingham, S.B., J.P. Volkmer, A.J. Gentles, D. Sahoo, P. Dalerba, S.S. Mitra, J. Wang, H. Contreras-Trujillo, R. Martin, J.D. Cohen, et al. 2012. The CD47-signal regulatory protein alpha (SIRPa) interaction is a therapeutic target for human solid tumors. *Proc. Natl. Acad. Sci. USA.* 109:6662–6667. https://doi.org/10.1073/pnas.1121623109

Xu, M.M., Y. Pu, D. Han, Y. Shi, X. Cao, H. Liang, X. Chen, X.D. Li, L. Deng, Z.J. Chen, et al. 2017. Dendritic Cells but Not Macrophages Sense Tumor Mitochondrial DNA for Cross-priming through Signal Regulatory Protein α Signaling. *Immunity.* 47:363–373.e5.

Yazawa, K., M. Fujimori, T. Nakamura, T. Sasaki, J. Amano, Y. Kano, and S. Taniguchi. 2001. Bifidobacterium longum as a delivery system for gene therapy of chemically induced rat mammary tumors. *Breast Cancer Res. Treat.* 66:165–170. https://doi.org/10.1023/A:1010644217648

Yu, T., F. Guo, Y. Yu, T. Sun, D. Ma, J. Han, Y. Qian, I. Kryczek, D. Sun, N. Nagarsheth, et al. 2017. Fusobacterium nucleatum Promotes Chemoresistance to Colorectal Cancer by Modulating Autophagy. *Cell.* 170:548–563.e16.

Zhou, S., C. Gravekamp, D. Bermudes, and K. Liu. 2018a. Tumour-targeting bacteria engineered to fight cancer. *Nat. Rev. Cancer.* 18:727–743.

Zhou, L., M. Zhang, Y. Wang, R.G. Dorfman, H. Liu, T. Yu, X. Chen, D. Tang, L. Xu, Y. Yin, et al. 2018b. Faecalibacterium prausnitzii Produces Butyrate to Maintain Th17/Treg Balance and to Ameliorate Colorectal Colitis by Inhibiting Histone Deacetylase 1. *Inflamm. Bowel Dis.* 24:1926–1940.

Zitvogel, L., Y. Ma, D. Raoult, G. Kroemer, and T.F. Gajewski. 2018. The microbiome in cancer immunotherapy: Diagnostic tools and therapeutic strategies. *Science.* 359:1366–1370. https://doi.org/10.1126/science.aar6918

JEM

# Supplemental material

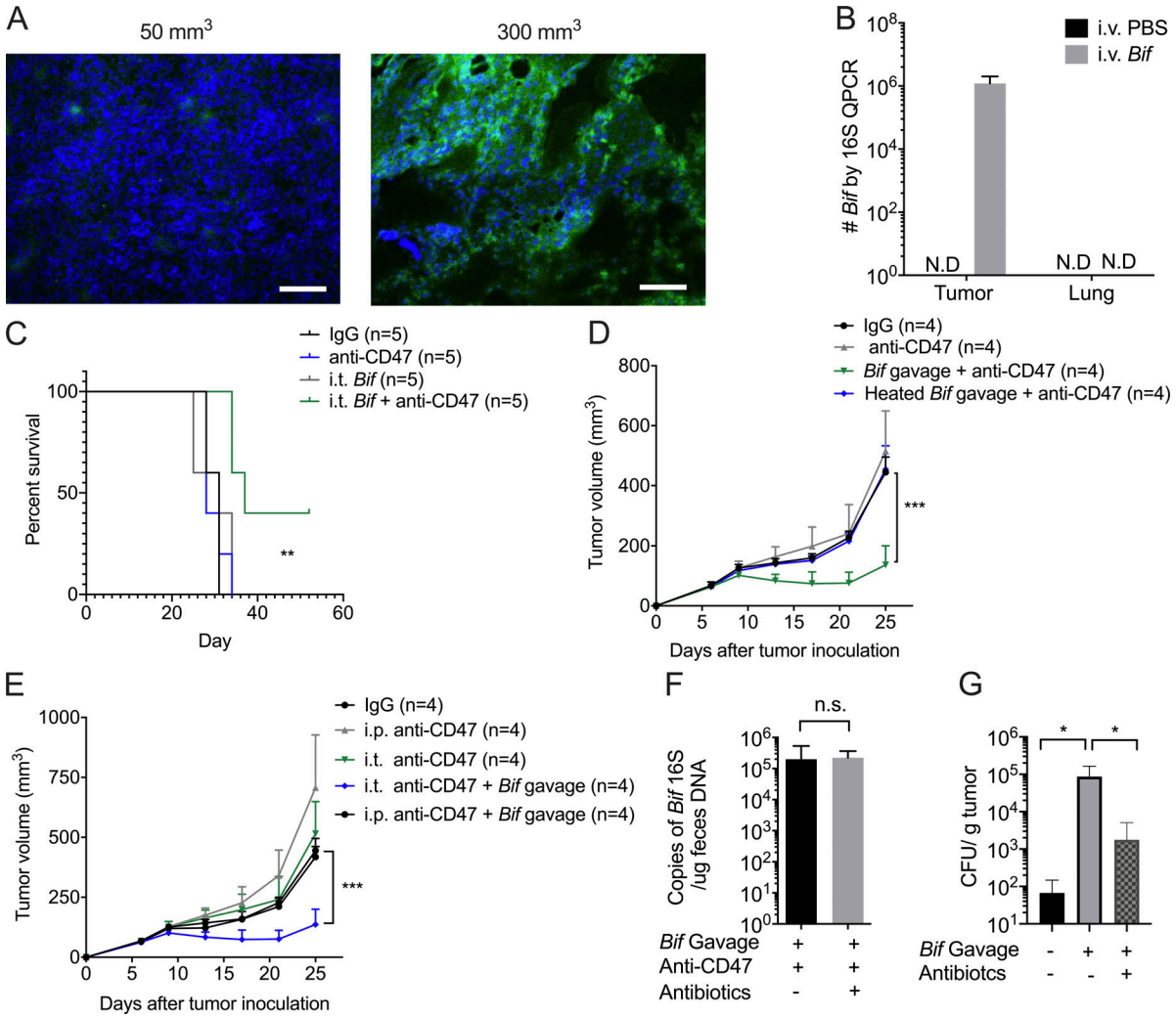


Figure S1. **Gut microbiota could survive in the hypoxic TME and prolong mouse survival.** Related to Fig. 2. **(A)** Representative image of HIF1α stain of different volumes of tumors. Immunofluorescence analysis of hypoxia: HIF1α (green) expression on different-volume tumor tissue slides. Tumor volume of the left: 50 $mm^3$; tumor volume of the right: 300 $mm^3$. Scale bars, 20 µm. One representative experiment is depicted from two experiments yielding similar results. **(B)** Accumulation of *Bifidobacterium* inside tumors but not lung sites after treatments. MC38 tumor–bearing Tac mice were i.v. injected with 1.5 × $10^7$ CFU *Bifidobacterium* or PBS three times when tumor size approaches 200 $mm^3$. 7 d later, tumor tissues were collected for qPCR detection of *Bifidobacterium*. One representative experiment from two experiments yielding similar results is depicted. N.D., not detected. **(C)** Survival curves of tumor-burden mice with different treatments. MC38 tumor-bearing Tac mice were i.t. injected with 70 µg anti-CD47 antibody (Ab) or 70 µg rat IgG on days 9 and 13, respectively. For i.t. injection of *Bifidobacterium*, mice were i.t. injected with 2.5 × $10^6$ CFU *Bifidobacterium* or PBS on days 6, 9, and 13. Mice were euthanized when the tumor size approached end points. The anti-CD47+ i.t. *Bifidobacterium* group is compared with the IgG group. One representative experiment from at least two experiments yielding similar results is depicted. **, P < 0.01 (log-rank test). **(D)** Heat-killed *Bifidobacterium* failed to facilitate CD47-based immunotherapy. Newly arrived Tac C57BL/6 mice were subcutaneously injected with 5 × $10^5$ MC38 cells. Each mouse was i.t. injected with 70 µg anti-CD47 Ab or 70 µg rat IgG on days 9 and 13, respectively. The mice with *Bifidobacterium* administration were gavaged with 5 × $10^8$ *Bifidobacterium* or heat-inactivated *Bifidobacterium* on days 6, 9, and 13. Tumor volume was measured at the indicated time points. ***, P < 0.001 (two-way ANOVA). **(E)** Oral administration of *Bifidobacterium* failed to facilitate antitumor efficacy after systemic administration of anti-CD47 antibody. Newly arrived Tac C57BL/6 mice were subcutaneously injected with 5 × $10^5$ MC38 cells. Each mouse was i.t. injected with 70 µg anti-CD47 Ab or 70 µg rat IgG on days 9 and 13 or i.p. injected with 500 µg anti-CD47 or rat IgG on days 9 and 13, respectively. The mice with *Bifidobacterium* administration were gavaged with 5 × $10^8$ CFU *Bifidobacterium* on days 6, 9, and 13, respectively. Tumor volume was measured at indicated time points. ***, P < 0.001 (two-way ANOVA). **(F)** I.t. antibiotics therapy does not reduce the *Bifidobacterium* copies in mouse feces. qPCR detection of *Bifidobacterium* in fresh feces collected from mice with indicated treatments on day 14 (also see Fig. 2 H; nonpaired Student's *t* test). **(G)** Detection of *Bifidobacterium* inside tumor tissues after *Bifidobacterium* gavage and i.t. antibiotics treatment. Newly arrived Tac C57BL/6 mice were subcutaneously injected with 5 × $10^5$ MC38 cells. For oral administration of *Bifidobacterium* (*Bif*), mice were gavaged with 5 × $10^8$ CFU *Bifidobacterium* or PBS on day 7, 10, and 13. Mice were i.t. injected with 100 µl antibiotic cocktail solution or PBS every other day from day 6. Tumor tissues were collected on day 17 and homogenized for anaerobic culture of *Bifidobacterium*. Presented as mean ± SEM. *, P < 0.05 (Mann–Whitney *U* test of log scale). n.s., not significant.

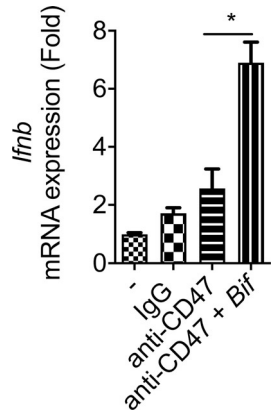


Figure S2. **Type I IFN could be up-regulated in bone marrow–derived DCs cocultured with tumor cells and *Bifidobacterium* after CD47 blockade.** Related to Fig. 3. qPCR of *Ifnb* mRNA levels in bone marrow–derived DCs. Bone marrow–derived DCs ($2 \times 10^6$) were cocultured with MC38 cells ($2 \times 10^6$) with 10 µg/ml anti-CD47 or 10 µg/ml rat IgG in the presence or absence of $2 \times 10^6$ *Bifidobacterium* for 8 h. DCs were then sorted out for *Ifnb* quantification by qPCR. Presented as mean ± SEM. *, $P < 0.05$ (nonpaired Student's *t* test).

**Table S1 is provided online as a Word document and shows the sources of all the reagents and resources used.**